

Development of a Numerical Toolbox for the Computer Aided Design of Composite Over-Wrapped Pressure Vessels

Eugenio Brusa¹ and Matteo Nobile²

Abstract: Lightness of high pressure vessels is currently assured by composite materials. Construction of over-wrapped composite pressure vessels with inner metallic liner is for instance compatible with standards requirements of the hydrogen technology of energy storage. Therefore a typical layout manufactured by some industries consists of a cylindrical vessel with covering of carbon-epoxy laminates and metallic impermeable liner. To allow the filament winding of the composite fibres are used hoop and helical layers, respectively. A single nozzle is usually built. It requires that the vessel material is reinforced. This need imposes to have a variable thickness in the composite layer. In practice, fibres orientation angle and thickness are both variable. These aspects make hard a straight design operation by means of analytical approaches. In this paper a numerical design toolbox is developed. It includes a preliminary definition of the fibres network, found by the so-called netting analysis, the theory of composite laminates and the structural optimisation through the Finite Element Method. An industrial prototype was used as a test case to validate the proposed approach. Burst and auto-fretage pressures for the liner were predicted and a preliminary analysis of the fatigue life was performed.

Keywords: High pressure vessel, Carbon fiber laminates; Finite Element Method; Filament winding.

1 Introduction

Emerging technologies aimed at converting and storing energy motivate the current demand of safe and light high pressure vessels to store large volumes of gas,

¹ Dept. Mechanics, Politecnico di Torino, Corso Duca degli Abruzzi, 24; 10129 Torino, Italy; email:eugenio.brusa@polito.it

² Former student, nowadays Engineer at Danieli Officine Meccaniche, Buttrio (Ud), Italy; e-mail: m.nobile@danieli.it

e.g. compressed Hydrogen [Lark (1977); web(1)-(19); Aceves (2000); Tacheichi (2003); Jansenn (2004)]. Since they are used in transportation systems lightweight is a priority of the design operation. To fit this requirement over-wrapped composite pressure vessels are manufactured [Krikanov (2000), Parnas and Katirci (2002), Tam (2002), Vasiliev (2003), Ko (2005)]. An inner liner made of Steel, Aluminium or polymers is reinforced by the outer shell made of fibre reinforced composite material. Metals are currently still preferred for the liner, although polymers avoid the brittleness caused by the Hydrogen [web(4), (7), (18)]. Liner assures tightness, lightness and an easy manufacturing process. Geodesic ends reinforced by a filament winding of carbon fibres, with hoop and helical layers, assure the required uniform strength [Zickel (1962), Krikanov (2000); Jae-Sung (2002), Tam (2002); Cheol-Ung (2005)]. Nevertheless, design operation is rather difficult. The actual condition of slip and friction at the interface between the composite and metallic layers is unknown [Chang (2000). Kabir (2000)]. To allow the filament winding of the composite fibres are used hoop and helical layers, respectively [Cohen (1997); Cho-Chung (2000); Cheol-Ung (2005)]. A nozzle is designed to store the gas. It requires that the vessel material is reinforced in correspondence of the opening. Therefore a variable thickness in the composite layer is imposed [Cho-Chung (2000)]. Moreover, helical fibres have a variable orientation angle in the vessel heads to assure the equilibrium of the composite material [Zickel (1962); Sun (1999), Krikanov (2000)]. Analytical approaches were proposed to perform the stress analysis of the over-wrapped composite vessels [Chang (2000); Cho-Chung (2000); Cheol-Ung (2005); Jae-Sung (2002); Akbarov and Mamedov (2009)]. They simultaneously deal with the primary and secondary stresses foreseen by the standards [Fryer and Harvey (1997)]. Unfortunately they need to know at least the composite layout and the angle orientation of the helical fibres. In practice, for the design operation is rather difficult to implement a procedure only based on those analytical approaches, as it was demonstrated in [Kabir (2000)]. Nevertheless, current practice of the manufacturers may help the development of a numerical toolbox for the vessel design. They are used to define preliminarily the layout of the composite fibres network, by means of the so-called "netting analysis" [Krikanov (2000)]. A rough prediction of the fibre orientation angle in the composite layer is found by supposing that the material strength is only assured by the fibres. The contribution of the composite matrix is just considered in terms of volume [Cohen (2001)]. Currently, design is only based on this step and a vessel prototype is usually built up and then tested [web(2,13-16)]. Burst pressure and fatigue tests allow the manufacturer refining the vessel geometry by a sort of trial-and-error approach [Sih (1986); Kam (1997); Sun (1999); Chang (2000); Parnas (2002)]. It looks effective at the end of the procedure, but the number of tests performed is too large. This approach is too expansive. In this paper, an alternative method is

developed. Netting analysis is quickly implemented to have a preliminary definition of the composite parameters. Theory of composite laminates is then applied to complete the composite layout design. Finite Element Method (FEM) is finally applied to study all the localized stress concentration and the fatigue behaviour of the whole vessel, where the composite covering interacts with the metallic liner [Tam (2002)]. This method was implemented in MATLAB (©The Mathworks) and interfaced with the ANSYS© code. An industrial prototype was built and analysed to perform a preliminary experimental validation of the proposed approach. Actually, the static behaviour, the autofrettage and burst pressures were correctly predicted. A structural optimisation of the prototype was evenly performed. Prediction of the fatigue life of the metallic liner was set up, but it still needs for an assessment based on more experimental results.

2 Design criteria and vessel layout

Design criteria for the composite vessel are defined by the ISO 11439 [ISO (2000)] and ASME Sec.X [ASME (2007)] standards, respectively. Few important ratios will be here recalled since they will be used in the implementation of the design algorithm. Pressure values have to fit these requirements:

$$\frac{p_b}{p_s} \geq 2.35; \quad \frac{p_c}{p_s} = 1.25. \quad (1)$$

where p_b is the burst pressure, p_s the service pressure, maximum value at which the gas is stored and p_c is the peak of the cyclic loading pressure, applied in case of the fatigue test. Safety factor is defined by means of the so-called “stress factor”:

$$n = \frac{\sigma_{\max, \text{fibre}}(p_b)}{\sigma_{\max, \text{fibre}}(p_s)} \quad (2)$$

where $\sigma_{\max, \text{fibre}}$ is the maximum value of stress acting on the composite fibre corresponding to the pressure indicated within the brackets. This factor is 2.35 for the carbon fibre composite [ISO (2000)]. In the over-wrapped composite pressure vessel, mechanical strength is assured by the outer cover, built by the filament winding technique [Cohen (1997)]. Hoop fibres are oriented up to 88° - 90° with respect to the shell meridians and helical fibres are usually deposited as two superimposed layers, whose orientation with respect to the meridians is $\pm\alpha$. Carbon fibre assures the strength of material, while the epoxy matrix allows a good adhesion with the fibres. Tightness is the main role of the liner. Welded joints are avoided. Hot rolling process is used to build heads and nozzles. Low alloy steels are preferred. In case of the Hydrogen technology they are tested in the related atmosphere, to evaluate the embrittlement effect [Parnas and Katirci (2002)]. Basically the vessel layout is

depicted in Fig.1. Main design parameters are the liner outer diameter, D , the outer and inner diameters of the nozzle, D_b and d , respectively, and the shell length, L . Design requirements are the volume, V , and the service pressure, p_s .

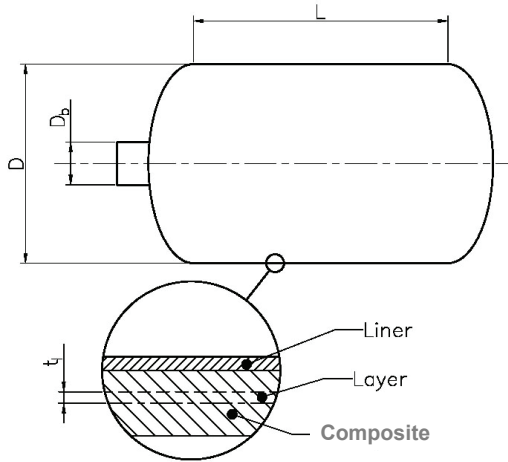


Figure 1: Design parameters of the over-wrapped composite pressure vessel

3 First step: netting analysis and preliminary composite layout

3.1 Equations

To have some required geometric parameters to implement the theory of composite laminates, the so-called “netting analysis” is performed [Zickel (1962)]. Vessel is supposed to be covered by a network of fibres and pressurized. Static equilibrium among fibres actions is then imposed. Composite material is assumed to be a continuum, where loading direction and material mechanical properties are those of the fibres [Ochoa and Reddy (1992); Cohen (2001)]. Only membrane stresses can be computed [Jones (1986); Ko (2005)] Axis-symmetry allows computing two principal stresses, i.e. along meridians, σ_m , and along parallels, σ_t . Laplace’s equation correlates those stresses [Fryer and Harvey (1998); Timoshenko (2000)]:

$$\frac{p}{t} = \frac{\sigma_m}{r_m} + \frac{\sigma_t}{r_t} \tag{3}$$

being p the pressure, t the thickness, r_m and r_t the shell radius in the meridian (π_m) and parallel (π_t) planes (Fig.2). To solve the problem, a second equilibrium equation is written along the direction of the symmetry axis [Harvey (1985)]. These

stress components allow computing easily those acting along the fibres, whose orientation is described by angle α . To allow the accessibility to the liner surface in deposition, α can not be constant along meridians. To avoid any accidental slip in deposition process [Cho-Chung (2002); Cheol-Ung (2005)], α is found by imposing null tangential stresses on the vessel surface. This assumption corresponds to a stable equilibrium of the deposited fibres, even in presence of resin.

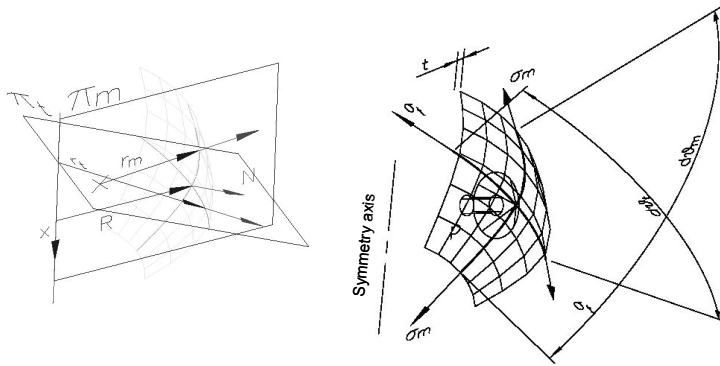


Figure 2: Principal planes (left) and stresses (right) defined of a generic infinitesimal portion of the vessel shell.

Fibres are loaded only by tensile stress. Stress is assumed to be constant along their length to assure a uniform strength. These two conditions of a null tangential stress and a pure tensile stress on the fibres were applied by Clairaut to compute angle α as follows [Zickel (1962)]:

$$R \cdot \left(R \frac{d\vartheta}{ds} \right) = C \Rightarrow R \cdot \sin \alpha = C = const. \quad (4)$$

For a given position on the vessel shell, R is the local radius of the vessel measured in the meridian plane (Fig.3). Reference frame depicted in Fig.3 assumes that z is the symmetry axis. Curvilinear coordinate s is used to follow the path described by the helical fibre. Angle α is the orientation from the meridian direction. It is fixed for a given value of R , being C a constant. Condition $\alpha=90^\circ$ corresponds to the hoop fibres, winded only on the cylindrical shell. In this case C is equal to R . Angle φ describes the angular position in the parallel plane, while angle ϑ is used to localize the fibre in the meridian plane. The local curvature of the fibre is described by radius r_t , being measured in a plane containing both the fibre and the origin of

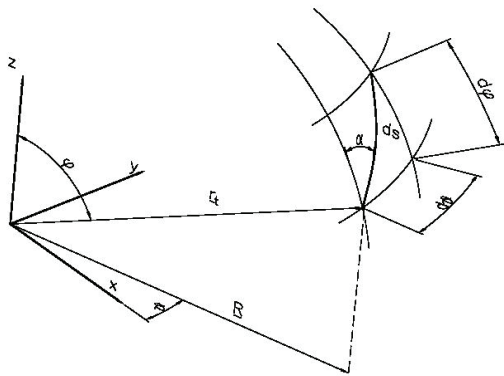


Figure 3: Reference frame and coordinates used in the netting analysis to describe a composite fibre loading.

the reference frame. It does not corresponds to neither of the coordinated planes of the vessel, since the fibre is skewed.

3.2 Shell

Cylindrical shell includes layers with two plies and is built with two laminates [Jones (1986)]. A sketch is proposed in Fig.4. Equilibrium equations on the com-

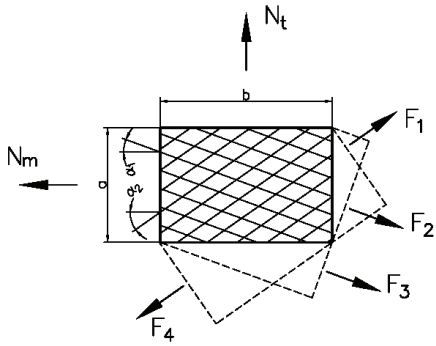


Figure 4: Actions applied to the composite layer.

posite material are written for the two layers as follows [Jones (1986); Sih (1986)]:

$$\begin{aligned}
 N_m &= \sum_{i=1}^2 2 \cdot N_{f_i} \cdot \cos^2(\alpha_{c_i}) \\
 N_t &= \sum_{i=1}^2 2 \cdot N_{f_i} \cdot \sin^2(\alpha_{c_i}) \\
 \sigma_m &= \frac{p \cdot R_c}{2t_{layer}}; \quad \sigma_t = \frac{p \cdot R_c}{t_{layer}}; \\
 N_m &= \sigma_m \cdot t_{layer} = N_t/2
 \end{aligned} \tag{5}$$

In Eq.(5) the composite layer thickness is t_{layer} , R_c is the cylinder radius, N are the loads acting along the meridians, (N_m), the parallels (N_t) and the fibres (N_f). Fibre angles in the two laminates, referred to as 1 and 2, respectively, are $\alpha_{c1} = -\alpha_{c2} = \alpha_c$. Angle α_c is constant on the whole cylinder. Solution of Eq.(5) gives an optimal value of α_c equal to 54.74° , being assuring a stable equilibrium. Unfortunately, nozzle obliges varying α_c near to the opening to allow winding the fibres [Lark (1977)]. In practice, the manufacturing process leads to have even on the cylindrical shell a lower value of α_c than the optimal value above computed near the nozzle. Strength of layers looks therefore higher along the meridians. Hoop layers are introduced to reinforce the structure. Analysis is performed for two layers including both the hoop (1) and helical (2) fibres. Loads are N_{f_i} and fibre orientation α_{c_i} . In this case equilibrium is given by [Jones (1986)]:

$$\begin{aligned}
 N_t &= 2N_{f_1} \cdot \sin^2(\alpha_{c_1}) + 2N_{f_2} \cdot \sin^2(\alpha_{c_2}) \\
 N_m &= 2N_{f_1} \cdot \cos^2(\alpha_{c_1}) + 2N_{f_2} \cdot \cos^2(\alpha_{c_2}) \\
 2 \text{ layers} &\Rightarrow N_{f_1}, \alpha_{c_1}, N_{f_2}, \alpha_{c_2}
 \end{aligned} \tag{6}$$

Angle α_{c1} in the hoop layer is set at 90° . Angle α_{c2} is chosen by considering the ratio between the diameters of the nozzle and the head, respectively. In practice, stress occurring in the fibre has to be compared to the strength of the material. Stresses in the fibres are therefore computed:

$$\sigma_{hel} = \frac{N_{f_{hel}}}{t_{ply,hel}} = \frac{2N_{f_{hel}}}{t_{layer,hel}}, \quad \sigma_{hoop} = \frac{N_{f_{hoop}}}{t_{ply,hoop}} = \frac{2N_{f_{hoop}}}{t_{layer,hoop}}, \quad t_{ply} = \frac{1}{2}t_{layer} \tag{7}$$

Subscript “*hel*” indicates helical component, while “*hoop*” corresponds to the hoop direction. Thickness values t_{ply} , t_{layer} introduced in above Eq.(7) correspond only to the fibre. Design operation has to define the complete thickness of the composite layer, by including the composite matrix. To obtain the total thickness the following

identity is imposed [Cho-Chung (2002)]:

$$t_{layer} \cdot n_{layer} = t_{tot,layer} \cdot V_f \quad (8)$$

V_f is the ratio between the volume of fibres and the total volume of the composite layer [Cohen (2001)]. Stresses can be written as a function of the total thickness:

$$\begin{aligned} \sigma_{hel} &= \frac{p \cdot R_c}{2 \cdot V_f \cdot t_{tot,layer,hel} \cdot \cos^2(\alpha_c)} \\ \sigma_{hoop} &= \frac{p \cdot R_c}{V_f \cdot t_{tot,layer,hoop}} \left[1 - \frac{1}{2} \tan^2(\alpha_c) \right] \end{aligned} \quad (9)$$

According to the Stress Ratio (SR) between the helical (σ_{hel}) and hoop stress (σ_{hoop}) imposed by the Standards a direct expression of the total thickness of each layer in the cylindrical shell can be found:

$$\begin{aligned} t_{tot,layer,hoop} &= \frac{p_b \cdot R_c}{\sigma_{cr,fib} \cdot V_f} \left[1 - \frac{1}{2} \tan^2(\alpha_c) \right] \\ t_{tot,layer,helical} &= \frac{p_b \cdot R_c}{2 \cdot SR \cdot \sigma_{cr,fib} \cdot V_f \cdot \cos^2(\alpha_c)} \end{aligned} \quad (10)$$

Typical values of SR are 0,6 to 0,8 [ISO (2000); ASME (2007)]. In the following example value 0,7 will be assumed. Above Eq.(10) includes the burst pressure, p_b , and the ultimate tensile strength of the fibres material, $\sigma_{cr,fib}$.

3.3 Head

Angle α_{c2} was found in the shell by imposing a constant and maximum stress for each point of the fibre. To apply this assumption evenly to the vessel head the geodesic shape is usually preferred [Cho-Chung (2002); Jae-Sung (2002)]. If the material is isotropic the spherical head satisfies this requirement, while in the case of composite over-wrapped vessel the corresponding shape has to be defined. This task is performed by completing the preliminary design based on the netting analysis. A reference sketch is depicted in Fig.5. Constant stress along the fibre corresponds to:

$$R \sin \alpha_c = const. \quad (11)$$

Since radius varies on the head it can be understood that even angle α_{c2} changes. It follows a determined law which can be found. It is known that at the pole of the

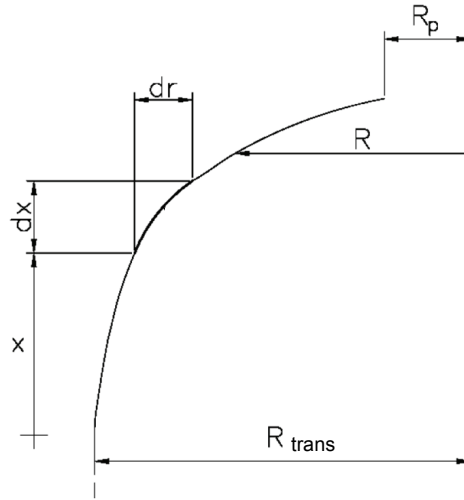


Figure 5: Layout of the geodesic head with upper nozzle.

head it is equal to 90° . Since it varies proportionally to the head radius up to the nozzle, having radius R_p :

$$\begin{aligned}\alpha_{c2} &= \arcsin\left(\frac{R_p}{R}\right) \\ \alpha_{trans} &= \arcsin\left(\frac{R_p}{R_{trans}}\right) \\ \alpha_{max} &= \arcsin\left(\frac{R_p}{R_p + 2B}\right).\end{aligned}\tag{12}$$

In practice, in Eq.(12) the first relation states that fibre angle at any point of the head is computed by inputting the local radius R and the nozzle radius R_p . There is a critical section of the vessel corresponding to the transition between the cylindrical shell and the head. The related angle is α_{trans} , while the local radius is R_{trans} . B is the winding bandwidth [Tam (2002)]. It is a typical process parameter. A maximum value is computed of α_{c2} in the last relation of Eq.(12). It is worthy remarking that to avoid a mathematical singularity a minimum value of the radius written at the denominator is introduced. It is suggested by the industrial practice [web(5)]. Stress concentration at the nozzle requires to increase the thickness. According to [Tam (2002); Ko (2005)] thickness t can be computed by imposing a constant flux

of fibres on the head and a constant stress on the helical fibre:

$$t = t_{trans} \cdot \left(\frac{\cos \alpha_{trans}}{\cos \alpha} \right) \cdot \left(\frac{R_{trans}}{R} \right) \tag{13}$$

This expression can be substituted in Eq.(9). After a long elaboration [Nobile (2005)], the dome shape can be found. For a given radius R , the dome coordinate x (Fig.3) is:

$$\frac{dx}{dR} = - \frac{1}{R_{trans}^3} \frac{R^3}{\sqrt{\frac{R^2 - R_p^2}{R_{trans}^2 - R_p^2} - \frac{R^6}{R_{trans}^6}}} \tag{14}$$

Above Eq.(14) can be difficultly integrated. Finite Difference Method (FDM) is usually necessary. This aspect makes very expensive computing the dome shape.

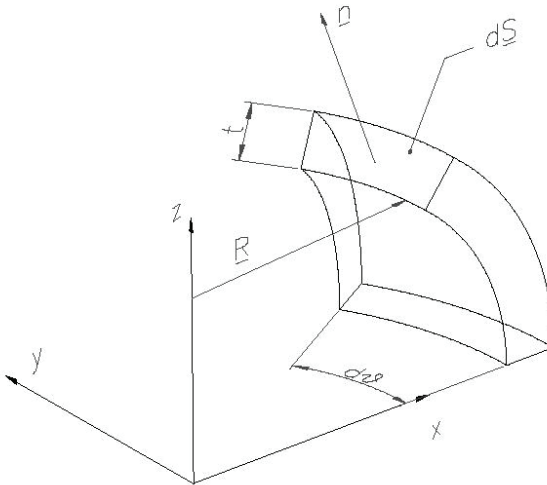


Figure 6: Analysis of the dome shape in the pressure vessel.

A faster solution is here originally implemented. In practice, the geodesic curve is locally approximated by arcs of circumference. In Eq.(3) radius r_t is approximated by the circumference radius:

$$p = \frac{N_m}{r_m} + \frac{N_t}{r_t} \quad r_t = \frac{R}{\sin(\varphi)} \tag{15}$$

while radius r_m is defined by substituting the above expression (15) into the equilibrium described in Eq.(5):

$$r_m = \frac{R}{\sin(\varphi)} \cdot \frac{1}{2 - \tan^2 \alpha} = \frac{R}{\cos(\vartheta_m)} \cdot \frac{1}{2 - \tan^2 \alpha} \quad (16)$$

To make easier the following discretization of Eq.(15) angle ϑ_m is introduced. It corresponds to the angular distance between r_i and R in Fig.3. Discretization is then operated as follows:

$$\begin{aligned} R_0 &= R_{trans} = R_c; \quad x_0 = 0; \quad \alpha_0 = \alpha_{trans}; \quad \vartheta_{m,0} = 0 \\ r_{m,i} &\cong r_{m,i-1} = \frac{R_{i-1}}{\cos(\vartheta_{m,i-1})} \cdot \frac{1}{2 - \tan^2(\alpha_{i-1})} \\ \Delta R_i &= r_{m,i} \Delta \vartheta_{m,i} \sin(\vartheta_{m,i-1}) \\ \Delta x_i &= r_{m,i} \Delta \vartheta_{m,i} \cos(\vartheta_{m,i-1}) \\ R_i &= R_{i-1} - \Delta R_i; \quad R_n = R_{min} = R_p + 2 \cdot B; \quad x_i = x_{i-1} + \Delta x_i \\ \vartheta_{m,i} &= \vartheta_{m,i-1} + \Delta \vartheta_{m,i} \\ \alpha_i &= \arcsin\left(\frac{R_c}{R_i}\right) \end{aligned} \quad (17)$$

Actually, few iterations allow drawing the dome shape. In practice, this approach achieves a result comparable to the FDM, but quite easier. The two solutions are almost superimposed, but in the case of the prototype here analysed the proposed approach required only 294 points instead of 10000 needed by the FDM.

4 Second step: composite layout refinement and stress analysis based on the theory of composite laminates

4.1 On the role of the composite matrix

Industrial practice demonstrates that in some over-wrapped composite pressure vessel the structural failure is detected in the composite matrix [Kam (1997); Chang (2000)]. Unfortunately, this event occurs even during the manufacturing process. It cannot be predicted by the netting analysis, since matrix structural contribution is neglected. This aspect needs of applying the theory of composite laminates [Jones (1986)]. It can be remarked that this theory can be easily applied after a preliminary design based on the netting analysis because the composite layout is already defined. Shell is firstly analysed. Material is orthotropic, on each layer, and the principal directions are identified by means of angle α . If a plane stress assump-

tion is made for the thin shell, the constitutive laws of material are [Jones(1986)]:

$$\begin{bmatrix} \sigma_1 \\ \sigma_2 \\ \tau_{12} \end{bmatrix} = \underbrace{\begin{bmatrix} \frac{E_1}{1-\nu_{12}\nu_{21}} & \frac{\nu_{21}E_1}{1-\nu_{12}\nu_{21}} & 0 \\ \frac{\nu_{12}E_2}{1-\nu_{12}\nu_{21}} & \frac{E_2}{1-\nu_{12}\nu_{21}} & 0 \\ 0 & 0 & G_{12} \end{bmatrix}}_{\mathbf{Q}} \cdot \begin{bmatrix} \varepsilon_1 \\ \varepsilon_2 \\ \gamma_{12} \end{bmatrix} \tag{18}$$

$$\Rightarrow \begin{bmatrix} \sigma_x \\ \sigma_y \\ \tau_{xy} \end{bmatrix} = \bar{\mathbf{Q}} \cdot \begin{bmatrix} \varepsilon_x \\ \varepsilon_y \\ \gamma_{xy} \end{bmatrix}$$

Directions 1,2 are principal and the stress components in a generic reference frame x,y can be obtained by applying a rotation α to matrix \mathbf{Q} , becoming $\bar{\mathbf{Q}}$, whose formulation is described in [Jones (1986)]. If the composite layers are symmetric and only the membrane stresses are considered, the related strains in the same reference frame are [Jones (1986)]:

$$\begin{bmatrix} \varepsilon_x \\ \varepsilon_y \\ \gamma_{xy} \end{bmatrix} = \mathbf{A}^{-1} \cdot \mathbf{N} \quad \mathbf{N} = \begin{bmatrix} N_x \\ N_y \\ N_{xy} \end{bmatrix}; \quad a_{ij} = \sum_{k=1}^n (\bar{Q}_{ij})_k (z_k - z_{k-1}) \tag{19}$$

$$\mathbf{N} = \begin{bmatrix} N_x \\ N_y \\ 0 \end{bmatrix} = \begin{bmatrix} N_m \\ N_t \\ 0 \end{bmatrix} = \begin{bmatrix} \frac{p \cdot R_c}{2} \\ p \cdot R_c \\ 0 \end{bmatrix}$$

In Eq.(19) n is the number of plies in the composite shell, z the coordinate of each interface between two plies, measured from the mid-plane. Bending effect is neglected, but on the cylindrical shell stress is constant, along the principal directions and the above model is applicable. Directions x and y correspond to the meridians and the parallels, respectively. Shear stresses, caused by the interlaminar actions, are not yet included, since in this model only the edges are loaded [Chang (2000)]. It is known that the complete equilibrium among the composite plies is assured by the interlaminar actions. They will be analysed at the next step by means of Finite Element Method [Kabir (2000)]. If the elastic properties to be inputted into Eq.(17) are not available, they can be found by applying the micromechanical model proposed by Halpin and Tsai, [Kardos (1990)]. Some new approaches were recently proposed for even worse cases, but it looked unpractical their implementation in this case [Guz et al.(2008), Guz and Dekret (2009)]. Composite material is damaged when a brittle rupture occurs within the fibres. Rupture occurs for different values of the load for each layer. A first critical stress referred to as “First Ply Failure (FPF)” causes the failure of the most loaded ply [Kam (1997)]. When even the last ply collapses the ultimate strength of material is achieved. Mechanical properties

of the composite material have to be defined by considering the gradual failure of the plies. The stress–strain curve depicted in Fig.7 gives an overview of the partial failure of plies. In particular, each ceiling corresponding to a constant stress value identifies the failure of one ply.

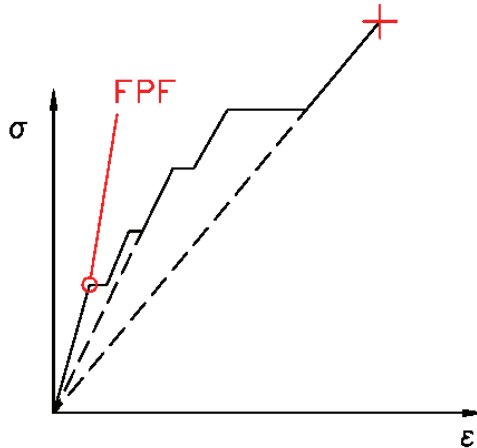


Figure 7: Stress computation in the geodesic head region.

It can be remarked that in case of pressure vessel used to store the hydrogen the role of the matrix has to be evaluated at different temperatures [Parnas and Katirci (2002)]. From the point of view of the burst pressure matrix can affect the maximum value of pressure allowed, because of the hoop effect played on the liner. It has a certain importance on the strength of the fibres, if a stiffening effect due to the biaxial tensile loading is applied, for higher values of pressure. In case of liquid and gas storage a long term period of loading is foreseen [Takeichi (2003); Janssen (2004)]. Temperature changes may be significant and sometimes very fast. Filling operation at low temperature could be critical [Aceves (2000)]. Carbon fibres look thermally stable, while the matrix may suffer the creep effect. These aspects are not yet included here, but they have to be further discussed in a future work. In this paper a preliminary stress analysis is performed to allow a preliminary structural design suitable to define some basic geometric parameters and the shape of the whole vessel. It looks suitable to identify the critical points of the vessel, in case of constant temperature. After this preliminary design both the thermo-mechanical and fatigue issues should be discussed.

4.2 Composite failure analysis

In the specific case of the hydrogen gas storage the metallic liner assures the vessel tightness. Design operation is therefore based on the ultimate strength of the composite material. A partial damage due to the rupture of some plies is somewhere accepted [Ko (2005)]. A critical issue for design is the selection of the failure criterion for the composite material. Zinoviev, Tsai-Wu and the Maximum Normal Stress are all proposed [Jones (1986); Sih (1986); Muscat (2003); Ziehl (2003)]. Manufacturers [web(3,5-8)] are prone to apply the Zinoviev's criterion [Sih (1986)]:

$$Z_{index} = \frac{\sigma_1}{X_t} \leq 1 \quad (20)$$

In practice, principal stress σ_1 and ultimate strength X_t along the fibre direction are compared. This criterion is one of the most easy to be implemented, but it looks less conservative than some others [Cheol-Ung (2005)]. It neglects the strength of material of the composite matrix. To have the possibility of comparing the results of all the above mentioned failure criteria, they were included by the authors into the numerical toolbox. In particular, it can be remarked that formulation of the Tsai-Wu criterion [ANSYS (2008)] requires a more difficult implementation, because of the number of parameters involved:

$$F_1 \sigma_1 + F_2 \sigma_2 + F_6 \tau_{12} + F_{11} \sigma_1^2 + F_{22} \sigma_2^2 + F_{66} \tau_{12}^2 + F_{12} \sigma_1 \sigma_2 \leq 1 \quad (21)$$

$$F_1 = \frac{1}{X_t} + \frac{1}{X_c}; \quad F_2 = \frac{1}{Y_t} + \frac{1}{Y_c}; \quad quad F_6 = \frac{1}{S_t} + \frac{1}{S_c};$$

$$F_{11} = -\frac{1}{X_t X_c};$$

$$F_{22} = -\frac{1}{Y_t Y_c}; \quad F_{66} = -\frac{1}{S_t S_c}; \quad F_{12} = -\frac{1}{2\sqrt{X_t X_c Y_t Y_c}};$$

In above Eq.(21) a plane stress state characterized by normal stress components σ_1 and σ_2 and shear stress τ_{12} is defined [Jones (1986)]. Symbol 1 is used to indicate the direction of the fibre, while 2 is orthogonal to the fibre, in the plane. Symbols X, Y and S are introduced to describe the strength of material in different tests. Longitudinal loading condition gives the ultimate strength X, while Y is used for the lateral loading and S for the shear test. Subscript t indicate tensile test, while c is used for compression.

5 Implementation into the MATLAB© code

This approach based on a modified formulation of the so-called “netting analysis” and on the theory of composites laminates was implemented by the authors

in MATLAB®. A new toolbox was built. Main inputs are the liner and nozzle diameters, shell length, layer thickness, ultimate strength of the fibre's material, volume V_f , pressure, safety factor, stress factor (SR) and filament winding bandwidth, B . Outputs are the burst pressure, actual ultimate strength, theoretical and actual thicknesses and number of helical and hoop layers, deposition angles, mean stress on the geodesic dome, length of the vessel, shell and heads and the volume. The input menu is shown in Fig.8. For the industrial test case analysed the geodesic head shape was found and is depicted in Fig.9.

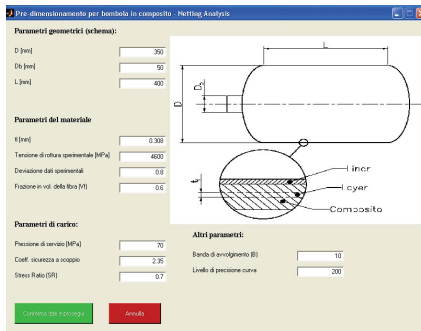


Figure 8: Example of the input menu interface of the toolbox developed by the authors (descriptions in Italian).

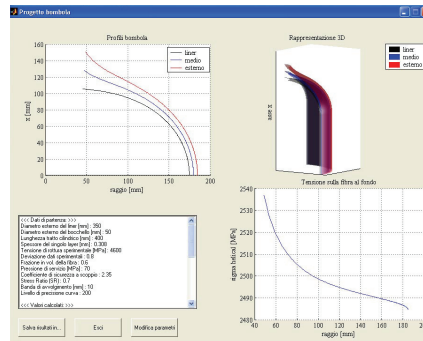


Figure 9: Example of the toolbox output, including (reading clockwise) the dome profile, a 3D perspective, stress acting on the fibre and the numerical parameters of the vessel.

Some interesting results can be seen in Figs.10,11. In Fig.10 a zoom of the geodesic profile is shown. It can be seen the variable thickness between the liner and the dome. The orientation angle α is indicated. It grows up from the transition between the head and the shell (left) up to the nozzle (right). Stress in the fibre looks almost constant for different values of radius R , as it was assumed in the proposed model (Fig.11). It is interesting to see the final variation of the orientation angle α shown in Fig. 11. The above described second step of the design was implemented in MATLAB®. Toolbox requires the material properties and performs the structural analysis. Plane stress state is assumed. Interlaminar stresses are supposed null. Elastic properties are inputted ($E_1, E_2, \nu_{12}, G_{12}$) for both the fibre and the matrix, as well as the fibres volume. Strength of material for tensile and compressive loads, along directions X, Y are evenly introduced, together with the shear strength of material, S .

Some inputs come from the previous module: the shell ply thickness, the number

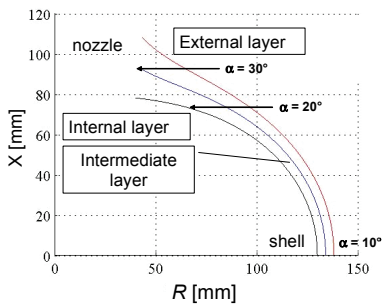


Figure 10: Layout of the geodesic dome computed by the toolbox.

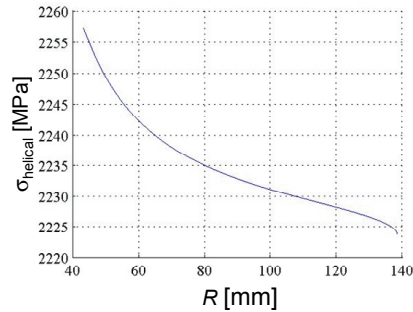


Figure 11: Stress computation in the geodesic head region.

of plies, the helical ply angle. Radius, pressure and safety coefficient are design requirements. Analysis of the composite layers proceeds in the toolbox by computing the collapse of each composite layer and variable mechanical properties are considered (Fig.7). The FPF value is computed. For each value of the applied load a subroutine verifies whether matrix is integer. Layers are usually assumed to be symmetric. Helical layer is located at the mid-plane, while hoop layers are upper and lower. The user can select a non-symmetric layout, with hoop layers at the outer radius of the shell. To assure the symmetry, plies are imposed to be multiple of four. Solution is iterative only if the gradual failure of the layers is required. Load distribution is updated, whenever a failure occurs in a ply. Tsai-Hill and Tsai-Wu criteria are applied to each layer. Stress, strain and failure criteria's coefficients are then computed for each ply. In case of time-variable stress, the maximum value is stored, for each layer. The ultimate strength of the composite material is computed by predicting the damage propagation, through the layers [Pahr and Bohm (2008); Patricio et al. (2009)]. When a matrix failure is detected stresses are computed by assuming the corresponding ply damaged and the stiffness matrix is updated [Kam (1997)]. Numerical outputs are available both as graphics and number lists. They are inputted into the FEM code for the following analysis of the whole vessel.

6 Third step: design of the whole vessel by means of the Finite Element Method

Previous steps of the design operation were aimed at defining a preliminary configuration of the composite vessel to allow a direct stress analysis by means of a FEM model. Because of the variability of the composite layers thickness and of the orientation angle the FEM code looks attractive to predict the mechanical behaviour of the coupled system composed by the cover and the liner [Krikanov (2000)]. Other

methods are currently applied in similar applications, e.g. BEM [Tan (2009)], or even new meshing procedures are proposed [Song and Chen (2009)]. They were considered unsuitable for this design activity because of either the lower precision in stress prediction or the intrinsic complexity of their implementation in this system. Stress concentration and edge effect at the transition between the shell and the head can be suitably analysed [Timoshenko (2000)]. A three-dimensional model is built, since this problem does not exhibit a complete axis-symmetry. All the basic parameters required to draw the vessel into the FEM code are directly supplied by the MATLAB© toolbox developed in this study. If the commercial code ANSYS© is used, elements like the 20-nodes brick can describe the vessel structure. In the case of the composite material option multilayer is switched on [ANSYS (2008)]. The elastic-plastic behaviour of the material of the liner has to be considered to predict the auto-fretting process. The Ramberg-Osgood curve is implemented and approximated by a bilinear curve [Dieter (1989)]. The goal of the FEM model is the refinement of composite thickness distribution and layers layout, the computation of the liner profile and of the autofretting pressure. Bending effects are included. Fatigue life can be predicted, provided that a suitable model for the failure mechanisms of both the composite and metallic material is applied. According to the Standards like ISO 11439 and ASME Sec.X this approach allows implementing the so-called “design by analysis” [Fryer and Harvey (1998)]. Critical points for the design operation are the nozzle neck and the edge between the shell and the head. These regions are therefore deeply studied.

6.1 Geometric modeling and meshing into the FEM code

Vessel geometry built through the MATLAB© toolbox usually includes hundreds of points which are unsuitable for an automatic meshing in the FEM code. Therefore a first action performed to transfer the results of the MATLAB© algorithm in the ANSYS© code is the interpolation by means of spline curves of the geometry previously computed. Model order is reduced. Geometry of the geodesic head is defined in the MATLAB© toolbox only up to radius R_{min} , corresponding to the part accessible by the filament winding process. It needs to be completed to describe the nozzle, by interpolating by a straight line the inner surface of the composite layer profile and by a cubic polynomial curve the outer one [Lee et al. (2008)]. This procedure defines some keypoints of the FEM mesh (cross symbols in Fig.12).

Thickness is computed as a difference among the coordinates of homologous points, on the outer and inner edge, respectively. Where the head is connected to the shell (at the so-called “transition region”) thickness decreases very fast, because there is the transition between the composite laminates of the cylinder, including both the hoop and helical layers and the head which embeds only helical layers. To keep the

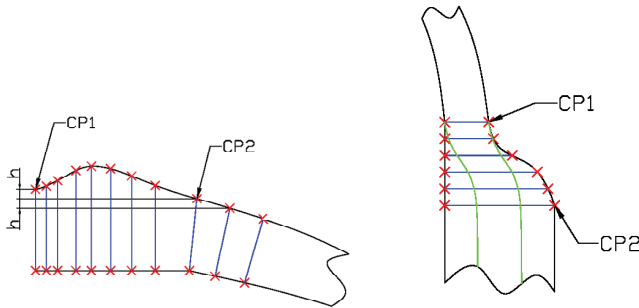


Figure 12: Keypoints generation in the transition region.

hoop reinforcement as close as possible to the region most affected by the bending effect and to make the transition sufficiently smooth a suitable ratio between the transition length along the meridians and the bandwidth B is usually looked for (Fig. 12) [Cho-Chung (2002)].

At the end of the above described procedure the liner geometry is defined. Shell thickness is constant, while in the head it is computed by imposing a constant volume of material, in condition of plastic deformation. In particular, the thickness of the head of the liner, t , is a function of the cylindrical shell radius, R_c , and thickness t_c , for a given radius R :

$$t = t_c \cdot \frac{R_c}{R} \quad (22)$$

When the vessel is actually thin, R is the same for the inner and outer profile, respectively. Solid vessel geometry is finally drawn by revolution, starting from the plane layout found. Following changes of the orientation angle α in the FEM model is made by defining its value element by element. It is constant within the element and corresponds to the average between the values assumed for the surrounding elements. This is an approximation of the actual layout. It looks rougher at the nozzle neck, where the gradient of angle α is steeper (Fig.13).

To decrease the computational time and assure a good approximation of the reality a regular mesh of hexahedral elements of the vessel eighth depicted in Fig.14 is used. Loads and constraints are then applied by resorting to the symmetry options.

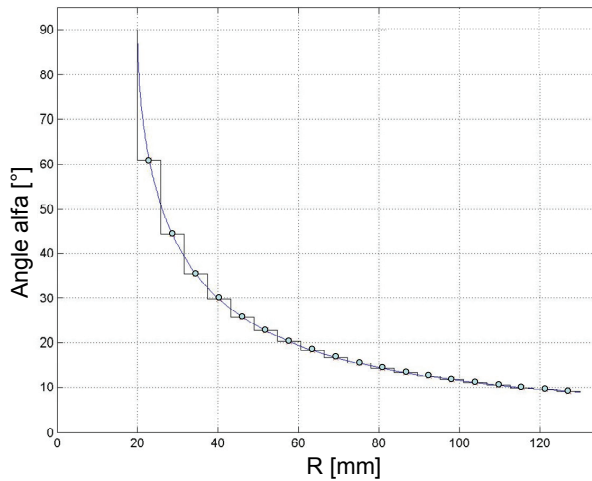


Figure 13: Example of comparison between the actual dependence of the orientation angle α on radius R (continuous line) and the FEM approximation (value for each element is indicated by the dark point).

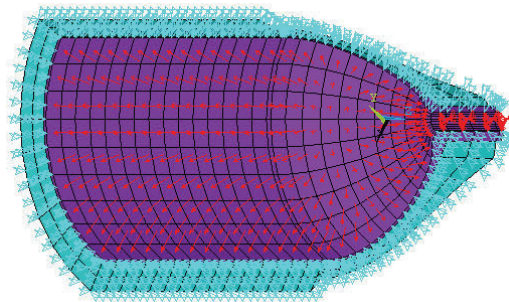


Figure 14: Example of FEM mesh of the vessel eighth with applied constraints and pressure.

6.2 Structure of the numerical toolbox

A flow-chart of the toolbox implementing the whole procedure is shown in Fig.15. It provides a file input to the FEM code. A first block (dashed) includes the netting analysis and the theory of composite laminates, while the second one performs the FEM discretization and pre-processing. A graphical interface requires coefficients, properties and strength of the composite material and the stress-strain curve

7 Numerical investigation and experimental validation on an industrial prototype

This research activity was motivated by the industrial need of optimising the composite structure of a pressure vessel currently manufactured. A preliminary development concerned the experimental validation of the numerical toolbox aimed at verifying the consistence of the numerical results in terms of stress and strain predicted. In a second step a preliminary optimisation of the vessel geometry was performed to propose a refinement of the product. The industrial prototype available for this operation has $D=260$ mm, $D_b=40$ mm, $d=23$ mm and $L=500$ mm (Fig.1) Thickness of the composite layer is 0.513 mm, while the percentage of volume for the fibres is 0.6. Strength of material for fibres is 3670 MPa and the filament winding bandwidth $B=10$ mm according to the supplier (Torayca T700). Service pressure is set at 70 MPa. Safety coefficient against the burst pressure is required to be 2.35 while the stress ratio is $SR=0.7$. Mechanical properties of materials used for the covering and of the liner, respectively, are listed in Table 1 and 2, while Table 3 includes some design parameters of the vessel geometry.

Table 1: Properties of the composite material Fiber FT700 SC 12K 50 C / Resine XB3585/XB3487

Single ply thickness (mm)= 0.2565
Single layer thickness (mm)= 0.513
Volume percentage of fibers $V_f=0.6$
$E_1=133200$ MPa; $E_2= E_3= 7870$ MPa
$\nu_{12} =\nu_{13} =\nu_{23}=0.27$; $G_{12} =G_{13} =G_{23}=4400$ MPa
$X_t=-X_c=2202$ MPa; $Y_t=-Y_c= Z_t=-Z_c=39.6$ MPa
$S=106$ MPa

7.1 MATLAB toolbox running

A preliminary analysis was performed by running the MATLAB© toolbox developed for this research activity. Some preliminary results were found. Burst pressure was computed as 164.5 MPa, while the critical stress was 3303 MPa. Layers thickness in [mm] were for the helical fibre 7.89 (theoretical) and 8.21(actual), for the hoop fibres 10.66 (theoretical) and 11.29 (actual). Number of helical layers were

Table 2: Properties of the Steel used for the liner

$E(\text{elastic})= 203000 \text{ MPa}; \nu= 0.3$ $E_2(\text{plastic})= 1583 \text{ Mpa}; \nu_{\text{plastic}}=0.5$ $\sigma_{\text{YIELDING}}=755 \text{ MPa}; \sigma_{\text{UTS}}=850 \text{ MPa}$

Table 3: Geometrical properties of the vessel

Geometrical properties of the vessel: Liner thickness= 2.5 mm Nozzle outer diameter= 40 mm Nozzle inner diameter= 23 mm Nozzle thickness= 8.5 mm Nozzle length=10 mm Bandwidth= 10 mm Length of the transition zone= 5 mm.

found 15.38 (theoretical) then approximated to 16, hoop layers were 20.78 (theoretical) and 22 (actual). Orientation angle was $\alpha=0.1545$ rad. The average value of stress on the head was found to be 2230 MPa. Geometry included the head whose length was 77.92 mm and the vessel long 655.85 mm. The whole volume was 32.65 litres. Since a direct design procedure is inapplicable [Kabir (2000)], FEM was used to verify the proposed layout. According to the flow-chart (Fig.15) all the geometrical data were inputted into the FEM model. The length of the transition region between the shell and the head, respectively, was assumed to be one half the width of the winding bandwidth of the hoop layers [Cho-Chung (2002)]. The inner diameter of the nozzle was defined by the dimensions of the threaded joint connecting the valve [Ko (2005)], while the outer diameter was computed by starting from the geometry of the profile. Manufacturer practice suggested a nozzle height of 10 mm. Safety coefficient for the liner was set at 2.35 with respect to the burst pressure [ISO (2000)]. The final layout of the liner was found by setting its thickness at 2.5 mm, to avoid buckling phenomenon and according to the practice [web(19)]. The selected value for the liner stiffness allows distributing the stress

better between the metal and the composite material. In presence of autofrettage this turns out in a good balance between the portions of load borne by the two materials in accordance to the results described in [Kabir (2000)]. In general it leads to have even a lower total weight.

7.2 FEM analysis in the ANSYS© Code

FEM discretization may be a rather difficult issue in this procedure, while the previous analyses are very easily performed by the MATLAB© toolbox. Meshing operation can be difficult where the thickness changes and the hoop layers plies stop. The so-called “transition region” between the shell and the head suffers the edge effect and the related stress concentration. Material can achieve the yielding in the liner. In this particular case the radial displacement is fairly larger in the head than in the shell, because of the presence of the hoop reinforcement in the cylinder (Fig.16).

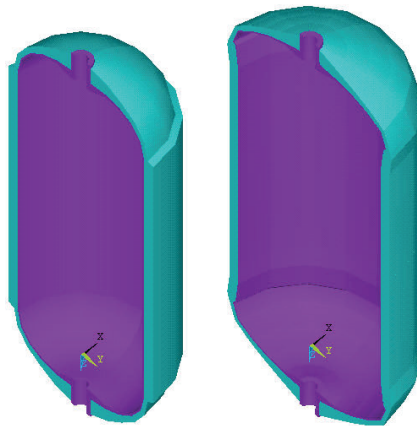


Figure 16: Comparison between the undeformed (left) and deformed (right) shape of the vessel under internal pressure.

Because of the number of degrees of freedom of the model a good compromise between the computational time and the accuracy of the solution has to be found [Chang (2000)]. A first investigation included 5 elements along the meridians and 5 along the parallels of the eighth of vessel analysed [Kabir (2000)]. This assumption allowed to have a fairly fast solution, but accuracy was insufficient. Actually this mesh looked too rough for several reasons. Geometry was only approximately

approximated by the distribution of elements. Liner exhibited the yielding of material at the edge between the shell and the head, but stress was found lower than the ultimate tensile strength everywhere. Radial displacement at the edge was very large (Figs.16 and 17). This could be motivated by the hoop effect exerted by the composite layers on the shell.

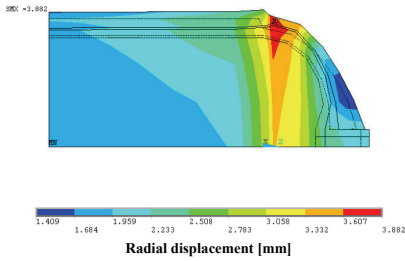


Figure 17: Radial displacement computation in the vessel according to the first coarse mesh operated.

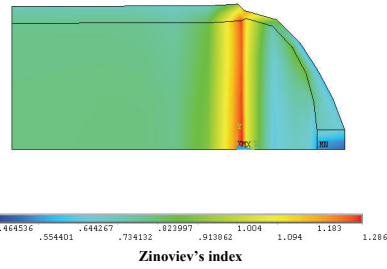


Figure 18: Distribution of the Zinoviev's coefficient defined in Eq.(20) on the vessel, according to the first coarse mesh operated. Failure occurs for values larger than one.

Stress looked lower at the nozzle than in the connection between the shell and the head, although there is a notch effect (Fig.18). This result could be justified by the increment of thickness which allows having a quite large portion of material around the nozzle region [Cho-Chung (2002)]. Composite material failed according to the Zinoviev criterion at the edge, but it was observed that the element solution disagreed with the nodal one. This effect is due to the large stress gradient monitored in the critical region. Tsai-Wu criterion confirmed the failure foreseen by Zinoviev's coefficient.

On the geodesic head a uniform stress distribution was found, according to the main assumption of geodesic shape [Zickel (1962)]. As it was expected the edge effect clearly affects the transition between the shell and the head. Some problems were detected in this first run. Radial stress was significant with respect to the circumferential and axial components, while it was supposed to be negligible. Shear stress in the radial-circumferential plane was found, but numerical values obtained for the unloaded part of the vessel could not be justified [Cheol-Ung (2005)]. All those results appeared not completely consistent with the basic assumptions of the model and somewhere incompatible with the daily practice of the manufacturer [web(5)]. Radial displacement at the edge between the head and the shell was

found equal to 3.8 mm, but it looked fairly larger than the measured value of 2.5 mm.

The experimental validation of the proposed model allowed realizing the main problem in the mesh. After few attempts it was found that a mesh including up to 10 elements along both the meridians and parallels, respectively, can achieve a good agreement with the experiments. Moreover, the same value of elements for the two directions allows having a good aspect ration in the finite element. Curvature of the region where elements are applied is also important. In particular, during the investigation it was found that a critical ratio can be described as:

$$\Psi_{cr} = \frac{D}{\text{subdivisions}} \quad (23)$$

In the case analysed a sort of threshold to assure a good aspect ratio corresponds to $\Psi_{cr}=30$ mm. The first mesh applied actually had $\Psi_{cr}=40$ mm. The second mesh introduced had $\Psi_{cr}=20$ mm, lower than the threshold. In this second run radial stress was found correctly null at the outer surface and opposite to the applied pressure at the inner surface [Timoshenko (2000)]. Liner exhibits a lower value of maximum stress, being justified by the larger number of elements. It still achieves the yielding at the edge between the shell and the head. Stress analysis depicted in Fig.19 is very interesting. Zinoviev coefficient is larger than one. This result confirms that the composite covering could fail. Moreover, across the thickness of the shell it can be detected a strong gradient of stress. Hoop layers are very stressed, but their role is consequently very important from the point of view of the material strength. Interlaminar stresses are then studied. They are present, mainly in the head region, while in the shell are practically null (Fig.20). This result is compatible with the theory of composite laminates applied in the first step of the analysis [Jones (2000)]. In this case radial displacement was compatible with the measured value.

7.3 Design of the optimized configuration of the pressure vessel

As far as the numerical investigation pointed out the preliminary design performed by means of the netting analysis and of theory of composite laminates cannot provide immediately a final layout suitable to assure the structural safety of the pressure vessel. Nevertheless, it allows performing a very fast preprocessing for the FEM model, which can be used to refine the design. Few tens of seconds are required to run the first two steps, while the FEM takes a longer time, e.g. some hours. In the test case only few attempts were sufficient to define the suitable number of elements required to have a good accuracy in the solution. To optimize the pressure vessel there are many design parameters which can be updated. In practice, a

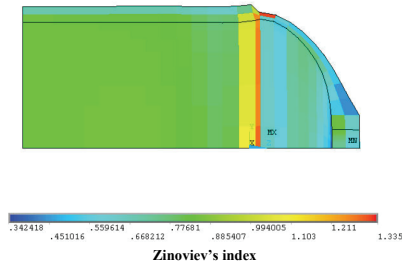


Figure 19: Distribution of the Zinoviev's coefficient on the vessel, according to the solution including a refined mesh. Values larger than one indicate the material failure.

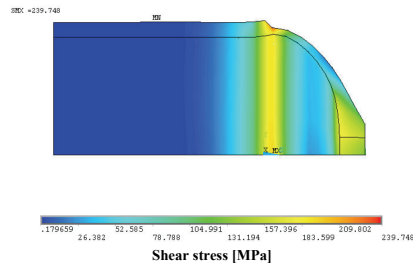


Figure 20: Shear stress distribution in the vessel found for the refined mesh case

straight proceeding suggests to change only the thickness of the liner and the composite layout. Furthermore, industrial practice says that below 2.5 mm liner may suffer the buckling effect [Tam (2002)]. Therefore this minimum value is usually fixed. Larger values may unsuitably increase the weight. Those remarks motivate why the manufacturer is prone to change only the composite layout and in particular the number of helical plies. To assure the safety of the pressure vessel composite layout was changed by modifying the number of helical plies. New configuration included 28 helical layers (56 plies) and 22 hoop layers (44 plies). Thickness of the helical layer was set at 14.36 mm, for the hoop layer at 11.28 mm and at 25.65 mm for the reinforcement. Zinoviev coefficient was then computed. It was 0.79 for the hoop layers and 0.32 for the helical layers on the shell. It became 0.9 on the transition region. Stress ratio appears decreased to 0.4 from 0.7. A fissuration along the meridians is the most probable failure [Kam (1997)].

A final FEM investigation on the optimised layout was performed. A larger number of helical layers decreases the stress acting on the external hoop layers. Shear stress is almost null, thus confirming that the goal of no slip is suitably achieved. Maximum stress due to the edge effect is significantly lower even in the liner. Stress in the head is lowered. The most critical component becomes the shell. Even the maximum radial displacement looks decreased, to 2.388 mm.

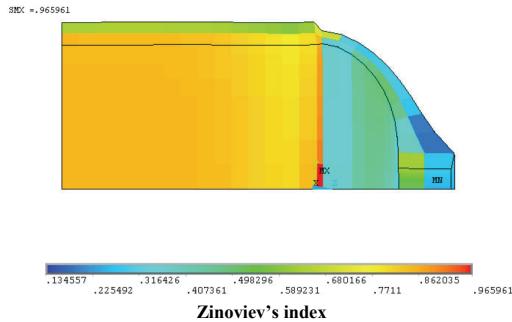


Figure 21: Distribution of the Zinoviev's coefficient on the vessel, according to the final design.

7.4 Autofrettage and fatigue

7.5 Computation of the autofrettage condition

A next step of the design operation was addressed. It concerned the computation of the stress in presence of the autofrettage phenomenon [Fryer and Harvey (1998)]. In practice, to increase the fatigue life of the liner a preliminary static loading is performed up to the yielding of the material of the liner at the inner radius. Residual compressive stresses at the inner surface of liner, where tensile stress is usually larger in operating condition allows decreasing the local effect of fatigue. Product life is increased. In practice, this process is aimed at operating the liner material in fatigue in the range of pressure $-p_{max}/2$ to $p_{max}/2$ instead of 0 to $p_{max}=1.25p_0$. The main problem, in predicting the actual autofrettage condition is that in this over-wrapped composite vessel the hoop effect superimposes to the liner strain. An analytical computation is only possible in case of metallic liner, without composite reinforcement [Fryer and Harvey (1998)]. FEM approach can be applied by simulating a so-called “pseudo-dynamic” analysis. A time history for the pressure is provided to the FEM code. At time t_1 pressure achieves p_{af} (autofrettage pressure lower p_b), at time t_2 it drops to zero, then, at time t_3 , it is increased up to p_c (first cycle in fatigue) as Figure 22 shows.

Those steps corresponds to a static loading up to the autofrettage condition, then to the unloading operation and finally to a loading up the maximum pressure applied in fatigue regime to the vessel. Static solution is found for each time step, being chosen long enough to avoid the dynamic effects [ANSYS (2008)]. In this implementation the toolbox requires a tentative value of p_{af} and the time-step. It computes the load history to be inputted into the FEM code. At each time step the

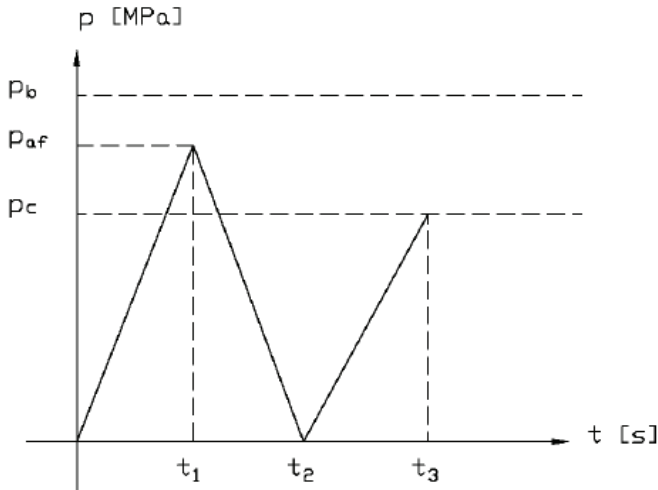


Figure 22: Time history of the pressure used in autofrettage operation.

FEM software computes the radial displacement, by including the plastic strain of the liner.

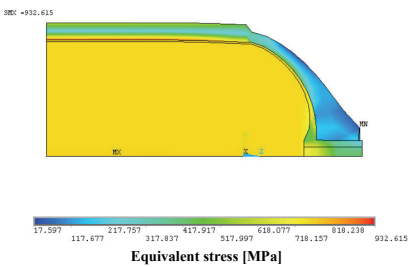


Figure 23: Stress distribution during the load step one corresponding to the autofrettage.

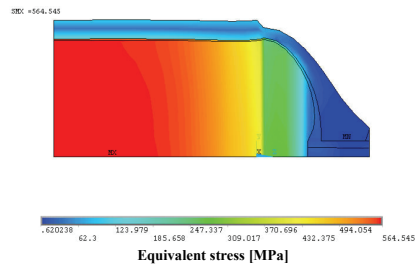


Figure 24: Residual stress distribution after the autofrettage.

In Fig.23 is shown the loading condition in terms of stress during the first step. It is remarkable that the liner is the critical layer. Computation of the residual stress (Fig.24) demonstrates that shell is more affected by the autofrettage phenomenon. Residual stresses occur more at the shell than at the geodesic head, because of the hoop reinforcement. In Fig.24 this condition is described through the equivalent stress, although it consists of the superposition of negative (compressive) principal

stresses. Stress analysis allowed defining the most suitable value of p_{af} . In principle if it is fairly large the mean stress in fatigue is lower [Suresh (1998)]. It cannot be increased too much because of the burst pressure. A compromise between those two limits was looked for. Since relation between mean value of stress and autofrettage pressure is nonlinear [Nobile (2005)], in practice an optimal value is slightly higher than p_c . In the test case it was 92 MPa ($p_c = 87.5$ MPa). The most important nodes to define p_{af} are located at the shell, the edge and the nozzle. Table 4 shows some results for those locations. Mean stress looks higher at the transition region and nozzle (head). Fracture occurs always at the liner shell, according to the experiments.

Table 4: Stress and fatigue analysis

Location	Shell	Edge	Head / Nozzle
σ_{max} [MPa]	698	708	717
σ_{min} [MPa]	-631	-290	-40
σ_{mean} [MPa]	33	209	340
$\sigma_{alternate}$ [MPa]	664	500	378
n_I cycles	11885	18492	85441
n_{II} cycles	17756	51954	82971

It is interesting seeing that composite layers during the autofrettage operation do not achieve the condition for failure, as it is documented in Fig.25. Liner shape changes after the autofrettage process, therefore Stress factor introduced in Eq.(2) is computed again. In the final configuration $n=2.75$, fairly higher than $n=2.35$ in the original case.

According to the ISO 11439 Standard, the industrial test case must assure a fatigue life of at least 3000 cycles, although the manufacturers are prone to increase this number up to 10000. This requirement is usually checked by means of fatigue tests [Suresh (1998)] directly performed on the prototype, a conventional pressure of $1.1p_s$. To complete the implementation of the design operations into the numerical toolbox some literature's models for low cycle fatigue were analysed [Dang Wang and Papadopoulos (1997); Susmel and Tovo (2007)]. Coffin-Manson, Smith, Watson and Topper are all applicable to the case of the liner. Multi-axial fatigue condition exhibiting a combination of fracture modes I and II, can be studied by

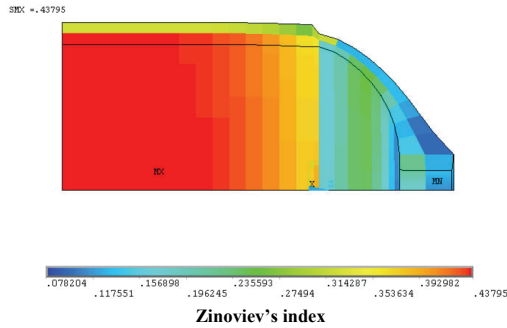


Figure 25: Distribution of the Zinoviev's coefficient on the vessel, during the autofrettage operation.

means of the Fatemi-Socie model [Suresh (1998); Susmel and Tovo (2007)]:

$$\begin{aligned} \varepsilon_{alt} \cdot \sigma_{max} &= \frac{(\sigma'_f)^2}{E} N^{2b} + \varepsilon'_f \cdot \sigma'_f \cdot N^{(b+c)} \text{ MODE I} \\ \gamma_{alt} \left(1 + S \frac{\sigma_{n,max}}{R_s} \right) &= \frac{\tau'_f}{G} N^{b_0} + \gamma'_f \cdot N^{c_0} \text{ MODE II} \end{aligned} \quad (24)$$

The variable strain ε_{alt} , occurring for the maximum stress σ_{max} , is related to the number of cycles N , through the Young's modulus E , the reference strain ε'_f and stress σ'_f in fatigue test and coefficients b, c , found by experiments [Suresh (1998)]. Shear variable strain γ_{alt} , at a given maximum stress, $\sigma_{n,max}$, acting orthogonally to the plane where failure occurs, is linked to cycles N , by experimental coefficients b_0, c_0, S and reference strain γ'_f , stress τ'_f and elastic modulus G . For the test case the approach agrees with the experimental results, when $\varepsilon'_f = 0.26$; $\sigma'_f = 948$ MPa; $b = -0.092$, $c = -0.445$, $\gamma'_f = 0.413$, $\tau'_f = 505$ MPa, $b_0 = -0.097$, $c_0 = -0.445$, $S = 1.18$. Life cycles predicted by FEM investigation, n_I and n_{II} are shown in Table 2. These are compatible with the experiments on the industrial prototype. Nevertheless, fatigue behaviour prediction is so difficult that only this preliminary attempt to investigate this issue cannot be considered sufficient. It just demonstrated the possibility of extracting the stress values from the FEM results and inputting into a dedicated algorithm implementing some fatigue models available in the literature. A deeper investigation has to be performed. In particular all the material properties and coefficients used in Eq.(24) require an experimental testing of the material. This task can be even more difficult in case of brittleness increasing due to the Hydrogen.

7.6 Final layout

According to the proposed design procedure, the final layout of the vessel was drawn. Some parameters were fixed, e.g. the density of fibres ρ_f [kg/m^3]=1790, of matrix ρ_m [kg/m^3]=1300, the percentage of volume of fibres $V_f=0.6$, the overall density of composite ρ [kg/m^3]=1594 and of liner (steel) of $7860 \text{ kg}/\text{m}^3$. Weight of the whole vessel was evaluated to be 38.4 kg, consisting of 25 kg of composite and 13.4 kg of liner (Fig.26). The benefit of the composite over wrapping is evident. For the same burst pressure the metallic shell in the new layout is thick 27 mm instead of the 43 mm of the original configuration.

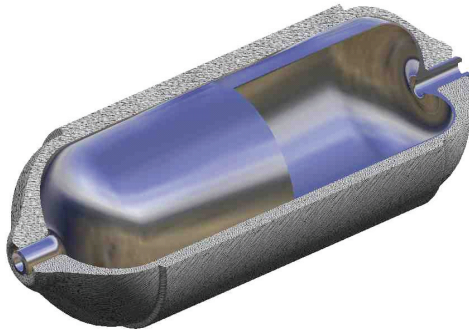


Figure 26: Final configuration of the vessel.

8 Conclusion

This paper is a result of the tight cooperation established between academy and industry aimed at looking for a suitable solution to a current need of pressure vessels manufacturers. A numerical approach is needed to decrease the costs of testing in the design operation of over-wrapped composite vessels. To fit the requirements of standards which need a detailed “design by analysis” for instance based on the FEM, a suitable approach was studied. Object is an over-wrapped composite vessels, with hoop and helical layers and inner steel liner. In practice industrial practice was followed in implementing a numerical toolbox in MAYLAB@ and ANSYS@ environments. A preliminary definition of the composite layers is found by following the so-called “netting analysis” and then refined by means of the theory of composite laminates. Outputs are used for pre-processing a FEM model. Structural analysis is then performed and a structural optimisation of the vessel design is obtained before prototyping. It can be remarked that the possibility of correctly predict the actual behaviour of a prototype of the pressure vessel was demonstrated.

Some problems related to the implementation were solved. The numerical toolbox allowed even a preliminary optimisation of the pressure vessel layout. Nevertheless, authors feel that this procedure is still immature for a straight application to the manufacturing process. Effects of temperature have to be modelled and suitably included, in particular for the Hydrogen technology. Fatigue needs to be properly investigated and modelled, particularly in the liner. This paper contributes to the state of the arts by describing a possible procedure to design at least preliminary the composite layout and the liner, while previous contributions only focused on the stress analysis of an existing layouts. The toolbox implemented demonstrated to achieve a fairly good agreement with the available experimental results. Nevertheless, an extensive investigation about temperature and fatigue effects in cooperation with an industrial manufacturer has to be performed. Experimental validation needs a fully instrumented vessel to investigate the local effects of stress.

Acknowledgement: Authors thank FABER – Industrie, Italy for supporting this work and particularly Mr. Alberto Agnoletti, M.Sc.Eng., and Mr. Jimmy Fabro, B.Sc.Eng., for sharing contents of the industrial practice and results of the experiments. For his kind suggestions [Susmel and Tovo (2007)] about the low cycle fatigue modelling in metals authors thank Prof. Luca Susmel, University of Ferrara, Italy.

References

Literature

- Akbarov, S.D.; Mamedov A.R.** (2009) “On the solution method for problems related to the micro-mechanics of a periodically curved fiber near a convex cylindrical surface”, *CMES: Computer Modeling in Engineering and Sciences*, 42 (3), pp.257-296
- Aceves, S.M.; Martinez-Frias, J.; Garcia-Villazana, O.** (2000) “Analytical and experimental evaluation of insulated pressure vessels for cryogenic hydrogen storage”, *Int. Journal of Hydrogen Energy*, 25, pp.1075-1085
- ANSYS® Releases 8.0, 9.0, 10.0, Reference Guides, 2004-2008.
- ASME Standard** (2007) *Boiler Pressure and Vessel Code SECTION X: Fiber-Reinforced Plastic Pressure Vessels*
- Chang, R.R.** (2000) Experimental and theoretical analyses of first-ply failure of laminated composite pressure vessels, *Composite Structures*, 49, pp.237-243
- Cheol-Ung, K.; Ji-Ho, K.; Chang-Sun, H., Chun-Gon, K.** (2005) “Optimal design of filament wound structures under internal pressure based on the semi-geodesic path algorithm”, *Composite Structures*, 67, pp. 443–452

Cho-Chung, L.; Hung-Wen, C.; Cheng-Huan, W. (2002) “Optimum design of dome contour for filament-wound composite pressure vessels based on a shape factor”, *Composite Structures*, 58, pp.469–482

Cohen, D. (1997) “Influence of filament winding parameters on composite vessel quality and strength”, *Composites Part A*, 28, pp. 1035-1037

Cohen, D.; Mantel, S.; Lyiang, Z. (2001) “The effect of fiber volume fraction on filament wound composite pressure vessel strength”, *Composites Part B*, 32, pp.413-429

Dang Van, K.; Papadopoulos I.V. (1997) *High cycle fatigue*, CISM Courses and Lectures n.392, Int. Centre for Mechanical Sciences, Springer, Wien New York

Dieter, G.E. (1989) *Mechanical metallurgy*, McGraw-Hill, Education, New York

Fryer, D.M.; Harvey, J. (1998) *High pressure vessel*, Chapman and Hall, New York.

Guz, A.N.; Dekret, V.A. (2009) “Stability Problem of Composite Material Reinforced by Periodical Row of Short Fibers”, *CMES: Computer Modeling in Engineering and Sciences*, 42 (3), pp.177-186

Guz, A.N.; Rushchitsky, J.J.; Guz I.A. (2008) “Comparative Computer Modeling of Carbon-Polymer Composites with Carbon or Graphite Microfibers or Carbon Nanotubes”, *CMES: Computer Modeling in Engineering and Sciences* 26 (3), pp.139-156.

Harvey, J. (1985) *Theory and design of pressure vessels*, Van Nostrand Reinhold, New York

ISO Standard (2000) *Gas cylinders – High pressure cylinders for the on-board storage of natural gas as a fuel for automotive vehicles*, ISO 11439

Jae-Sung, P.; Chang-Sung, H.; Chun-Gon, K.; Cheol-Ung, K. (2002) “Analysis of filament wound composite structures considering the change of winding angle through the thickness direction”, *Composite Structures*, 55, pp.63-71.

Janssen, H.; Bringmann, J.C.; Emonts, B.; Schroeder, V. (2004) “Safety-related studies on hydrogen production in high-pressure electrolyzers”, *Int. Journal of Hydrogen Energy*, 29, pp.759–770.

Jones, R.M. (1986) *Mechanics of composite materials*, McGraw-Hill, Washington

Kabir, M.Z. (2000) “Finite element analysis of composite pressure vessels with a load sharing metallic liner”, *Composite Structures*, 49, pp.247-255.

Kam, T.Y.; Liu, Y.W.; Lee, F. T. (1997) *First ply failure strength of laminated composite pressure vessels*, Elsevier Science, Amsterdam

Kardos, J.L. (1990) “Mechanical properties of polymeric composite materials,” in

E. Baer, A.Moet (eds.) *High Performance Polymers*, Hanser Publishers, Munich, pp. 199–251

Ko, W.L. (2005) “Structural analysis of Helios filament-wound tanks subjected to internal pressure and cooling”, NASA Scientific Reports Series on Advances in Aerospace and Aeronautics

Krikanov, A. (2000) “Composite pressure vessels with higher stiffness”, *Composite Structures* 48, pp.119-127

Lark, R.F. (1977) “Recent advances in lightweight, filament-wound composite pressure vessel technology”, NASA TM 73699.

Lee, K.; Wu, C.T.; Clarke, G.V.; Lee, S.W. (2008) “Computational Modeling of a Lightweight Composite Space Reflector using Geometrically Nonlinear Solid Shell Elements”, *CMES: Computer Modeling in Engineering and Sciences*, 33 (1), pp.109-129.

Muscat, M.; Mackenzie, D.; Hamilton, R. (2003) “A work criterion for plastic collapse”, *Int.Journal of Pressure Vessels and Piping*, 80, pp.49–58.

Nobile M. (2005) “Progettazione agli elementi finiti di recipienti in materiale composito per lo stoccaggio dell'idrogeno” (Design by FEM of composite pressure vessels for the Hydrogen storage), in italian, M.Sc. thesis, University of Udine, Italy.

Ochoa, O.O.; Reddy, J.N. (1992) *Finite Element Analysis of Composite Laminates*, Kluwer Academic Publishers, Dordrecht, pp. 111-128

Pahr, D.H.; Böhm, H.J. (2008) “Assessment of Mixed Uniform Boundary Conditions for Predicting the Mechanical Behavior of Elastic and Inelastic Discontinuously Reinforced Composites”, *CMES: Computer Modeling in Engineering and Sciences*, 34 (2), pp.117-136

Parnas, L.; Katranci, N. (2002) “Design of fiber-reinforced composite pressure vessels under various loading conditions”, *Composite Structures*, 58, pp.83–95

Patrício, M.; Mattheij, R., deWith, G. (2009) “Effects of the local structure on a cracked periodically distributed composite”, *CMES: Computer Modeling in Engineering and Sciences*, 41 (1), pp.69-93

Sih, G.C.; Skudra, A.M. (1986) *Failure mechanics of composites*, Elsevier Science Publishers B.V., Amsterdam, pp. 105-118

Song, R.; Chen, W. (2009) “An investigation on the regularized meshless method for irregular domain problems”, *CMES: Computer Modeling in Engineering and Sciences*, 42 (1), pp.59-70

Sun, X.K.; Du, S.Y.; Wang, G.D. (1999) “Bursting problem of filament wound composite pressure vessels”, *International Journal of Pressure Vessels and Pip-*

ing,76, pp.55-59

Suresh, S. (1998) *Fatigue of materials*, Cambridge University Press, Cambridge

Susmel, L.; Tovo, R. (2007) “A quantitative comparison among multi-axial fatigue criteria for low cycle fatigue”, Authors’ communication, Technical Report, Università di Ferrara, Italy.

Takeichi, N. et alii (2003) “Hybrid hydrogen storage vessel, a novel high-pressure hydrogen storage vessel combined with hydrogen storage material”, *Int. Journal of Hydrogen Energy* 28, pp.1121– 1129.

Tam, W.H., Griffin, P.S., Jackson, A.C. (2002) “Design and manufacture of a composite overwrapped pressured tank assembly”, Proc. AIAA-2002-4349 38th AIAA ASME SAE ASEE Joint Propulsion Conference and Exhibit, Indianapolis, Indiana, July 7-10, 2002

Tan, C. L.; Shiah, Y.C.; Lin, C.W. (2009) “Stress Analysis of 3D Generally Anisotropic Elastic Solids Using the Boundary Element Method”, *CMES: Computer Modeling in Engineering and Sciences*, 41 (3), pp.195-214.

Timoshenko S., (2000) *Theory of Plates and Shells*, McGraw Hill, New York

Vasiliev, V.V.; Krikanov, A.A.; Razin, A.F. (2003) “New generation of filament-wound composite pressure vessels for commercial applications”, *Composite Structures*, 62, pp. 449–459

Zickel J. (1962) “Isotensoid pressure vessels”, *ARS Journal*, pp.950-951

Ziehl, P.H.; Fowler, T.J. (2003) “Fiber reinforced vessel design with a damage criterion approach”, *Composite Structures*, 61, pp.823–829.

Websistes

web(1): Adoptech: www.adoptech.com

web(2): AIP: www.aip.org

web(3): Amalga: www.amalgacomposites.com

web(4): Dittmer, J.; Frost, S. : “A closer look at hydrogen”, www.machinedesign.com

web(5): Faber Industrie, Italy: www.faber-italy.com

web(6): Hexcel Composites: www.hexcelcomposites.com

web(7): Lincoln Composites Ltd. : www.lincolncomposites.com

web(8): McClean Anderson: www.mccleananderson.com

web(9): Petterson, J.; Hjortsberg, O. : “Hydrogen storage alternatives” available on www.tech.volvo.se

web(10): www.tifac.org

web(11): “Hydrogen Storage” www.fuelcellstorage.com

web(12):“Hydrogen storage materials”, www.aacg.bham.ac.uk/hydrogen

web(13): “Fuel Cell”, world.honda.com

web(14): Valenti, M.: “Filler up with hydrogen”, www.asme.com

web(15): www.qttww.com

web(16): “Composites”, web.nchu.edu.tw

web(17):“Pressure vessel and system design”, www.llnl.gov

web(18): “Manufacturing”, www.admc.aeat.co.uk

web(19): www.key-to-steel.com